X-Ray Resonant Raman Scattering: Observation of Characteristic Radiation Narrower than the Lifetime Width

P. Eisenberger and P. M. Platzman
Bell Laboratories, Murray Hill, New Jersey 07974

and

H. Winick
Stanford University, Stanford, California 94305
(Received 14 January 1976)

Intense tuneable synchrotron radiation was used to perform a high-resolution study of the resonant scattering response of Cu metal in the x-ray regime. One finds in the transition regime from fluorescence to resonant scattering that the linewidth of the emitted radiation becomes narrower than the lifetime-limited width of the fluorescent radiation.

Recently there has been considerable interest in the phenomena of resonant x-ray Raman scattering.[1-3] Experiments and theory have to date focused on the gross features of the phenomena. The experiments have all used low-resolution (~200 eV) detection systems while the theory has been one-electron in character and has not included the effects of the lifetime of the final state.

In this work we report very-high-resolution studies of resonant x-ray Raman scattering of copper in the resonant regime where lifetime considerations become very important. We find for the first time in the field of resonant Raman scattering, either in the visible or x-ray regime, the remarkable though understandable result that at resonance the energy width of the scattered radiation is ~30% less than the lifetime-determined width which is observed above resonance in the fluorescence regime. In addition we will show that one can uniquely identify the energy of excitation to the Fermi surface through this technique.

The experimental configuration is the same as described previously in Ref. 3, hereafter referred to as I, except that the solid-state detector was replaced by a double-silicon-(111)-crystal Bragg spectrometer which had an essentially Gaussian resolution function with a full width at half-maximum (FWHM) of 0.8 eV. The input radiation provided by the Stanford University storage ring SPEAR was monochromatized and made continuously tunable by a slit-channel-cut silicon-(220) spectrometer which had an essentially Lorentzian resolution function with a FWHM of 0.9 eV. This system provided about 10^{10} photons per second in the 0.9 eV bandwidth.

As in I the experiment was performed by first tuning the incident energy to a value in the vicinity of the K absorption edge of Cu ($\Omega_K + E_F = 8980$ eV). One then determines the spectrum of radiation scattered at 90° in the energy region around the $K\alpha_1$ fluorescence energy of Cu ($\Omega_K - \Omega_{L3/2} = 8048$ eV) by scanning the double-crystal Bragg spectrometer. The specific energy levels of copper that are involved are schematically indicated in Fig. 1. The signals were so weak (2 counts/sec at the peak of $K\alpha_1$ at resonance) that we decided to focus our attention on the $K\alpha_1$ region which has twice the signal of the $K\alpha_2$ region because the $P_{3/2}$ states have twice the degeneracy of the $P_{1/2}$ states.

The results for the dispersion of the peak (i.e., energy in versus energy out) and the linewidth

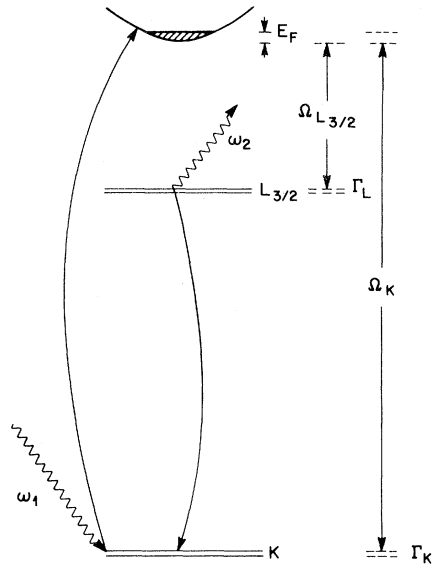

FIG. 1. Schematic of the energy levels of Cu involved in this study.

(FWHM) of the signal are summarized in Figs. 2(a) and 2(b), respectively. Absolute energies were not used because of the difficulty of calibrating the system absolutely to better than 1 eV. Thus the input energy, $\hbar\omega_1$, is measured relative to the resonant energy (i.e., $\Delta E_R = \hbar\omega_1 - \Omega_K - E_F$). The point $\Delta E_R = 0$ was fixed in a manner which will be described shortly. The output energy, $\hbar\omega_2$, was measured relative to the $K\alpha_1$ energy [i.e., $\Delta E_0 = \hbar\omega_2 - (\Omega_K - \Omega_{L_{3/2}})$] observed when the incident energy was far above threshold. The linewidth data are uncorrected for instrumental resolution effects. The expected linear Raman dispersion is observed [Fig. 2(a)] for energies below threshold and a minimum in the linewidth at resonance is also clearly seen [Fig. 2(b)]. In Fig. 3 we show the results for the absorption edge of copper (solid curve) observed in transmission and for the intensity of the observed scattered signal (dotted curve) uncorrected for the effects of the energy-dependent penetration depth of the incident beam. The two curves parallel one another remarkably well.

The notation used in the calculation which follows is the same as in I. The quantities Γ_K and Γ_L are the lifetime widths of the $1S$ and $2P_{3/2}$ holes, respectively. In the notation of I the one-electron scattering rate keeping only the resonant piece[3] is given by

$$\frac{dR(\omega_1,\omega_2)}{d\omega_2} = \left(\frac{\omega_2}{\omega_1}\right)\left(\frac{e^2}{mc^2}\right)^2 \frac{2c}{\pi}\int \frac{d^3k}{(2\pi)^3}(1-n_k)|M_{fi}|^2 \frac{\Gamma_L}{[\omega_1-\omega_2-(\epsilon_k+\Omega_{L_{3/2}})]^2+\Gamma_L^2}, \tag{1}$$

where

$$M_{fi} = \frac{\langle P|\vec{\mathrm{P}}\cdot\vec{\epsilon}_2|S\rangle\langle k|\vec{\mathrm{P}}\cdot\vec{\epsilon}_1|S\rangle}{m(\omega_1-\epsilon_k-\Omega_K+i\Gamma_K)}. \tag{2}$$

The states $|S\rangle$ and $|P\rangle$ are the one-electron wave functions characterizing the K and $2P_{3/2}$ shells while $|k\rangle$ and n_k are the corresponding wave function and occupation number for the conduction electrons. In the resonant region the $\vec{\mathrm{P}}\cdot\vec{\epsilon}$ matrix elements are slowly varying functions. In this case the integral

$$\int \frac{d^3k}{(2\pi)^3}(1-n_k) \equiv \frac{(2m^3)^{1/2}}{(2\pi)^3}\int_{E_F}^{\infty}\epsilon^{1/2}\,d\epsilon$$

may be replaced by an integral over $d\epsilon$ if we make the additional well-justified assumption for copper that Γ_K and Γ_L are small compared to E_F. With these assumptions the integral given in Eq. (1) can be performed exactly yielding

$$\frac{dR(\omega_1,\omega_2)}{d\omega_2} = C(\omega_1,\omega_2)\left\{\frac{\pi}{2}\frac{\Gamma_K+\Gamma_L}{\Gamma_K\Gamma_L A} + \frac{1}{AB}\left[\Delta E_0 \ln\left(\frac{\Delta E_R^2+\Gamma_K^2}{(\Delta E_R-\Delta E_0)^2+\Gamma_L^2}\right) + \left(\frac{\Delta E_0^2+\Gamma_L^2-\Gamma_K^2}{\Gamma_K}\right)\tan^{-1}\left(\frac{\Delta E_R}{\Gamma_K}\right) + \left(\frac{\Delta E_0^2+\Gamma_K^2-\Gamma_L^2}{\Gamma_L}\right)\tan^{-1}\left(\frac{\Delta E_R-\Delta E_0}{\Gamma_L}\right)\right]\right\}, \tag{3}$$

where $C(\omega_1,\omega_2)$ is a slowly varying function of ω_1 and ω_2 which contains the matrix-element effects and where $A = \Delta E_0^2 + (\Gamma_K+\Gamma_L)^2$ and $B = \Delta E_0^2 + (\Gamma_K - \Gamma_L)^2$. In I (i.e., poor-resolution experiment) we were only interested in the case $\Gamma_L = 0$.

Above threshold ($\Delta E_R \gg \Gamma_K + \Gamma_L$) Eq. (3) yields a Lorentzian fluorescence line centered at $\Delta E_0 = 0$ with FWHM of $2(\Gamma_K+\Gamma_L)$. For copper, theory[4] and experiment[5] roughly agree that $\Gamma_K \cong 0.74$ eV. It is these values we will use in our calculations. Below threshold ($\Delta E_R \ll -\Gamma_K - \Gamma_L$) Eq. (3) yields a spectrum with a sharp rise (width Γ_L) at $\Delta E_R = \Delta E_0$ followed by a $(\Delta E_0)^{-2}$ falloff to lower energies modulated by matrix-element effects. These results are described in more detail in I. In this paper we will focus our attention on the behavior of Eq. (3) in the neighborhood of resonance ($-\Gamma_K - \Gamma_L \leq \Delta E_R \leq \Gamma_K + \Gamma_L$).

To compare theory and experiment in the resonance regime, numerical evaluation of Eq. (3) was made to obtain the predicted shape and position of the scattered radiation for each value ΔE_R in the region of interest. The results are summarized in Figs. 2(a) and 2(b), where they are compared with the experimental results. The value of the incident energy which corresponds to $\Delta E_R = 0$ was chosen by matching the change in slope of the theoretical and experimental dispersion curves. The choice of zero would indicate that the Fermi surface in copper is located at the point of inflection in the K absorption curve for copper found in transmission (Fig. 3). This represents about a 2-V shift to lower energy from

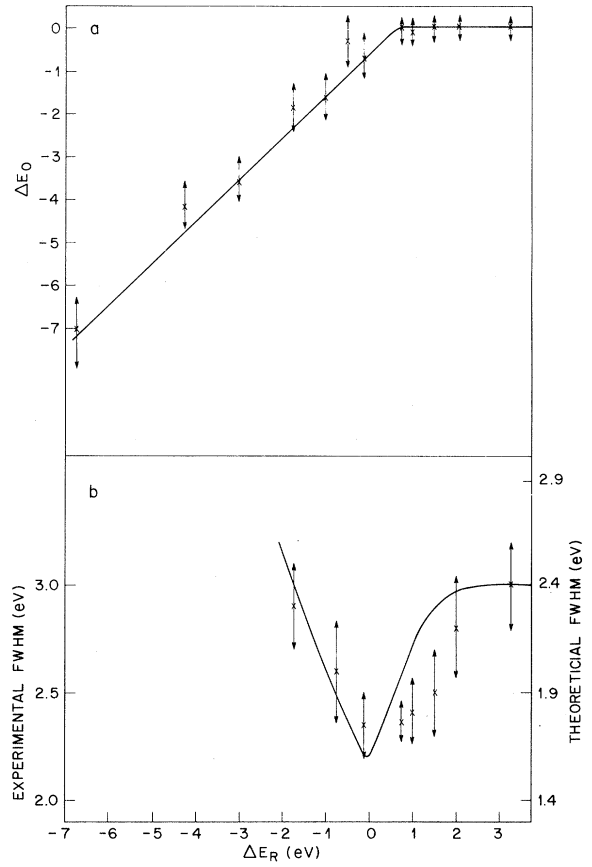

FIG. 2. Comparison of experimental results (points) with theoretical calculations (line) based on Eq. (3) for (a) the dispersion and (b) the linewidth of 90° scattered radiation as a function of ΔE_R. Note the separate scales for the theoretical and experimental linewidths. A value of 3.0 ± 0.1 eV for the experimentally measured $K\alpha_1$ linewidth was determined for $\Delta E_R \gg 0$.

the location determined by the low-resolution studies.[3] One should note that at $\Delta E_R = 0$ the centroid of the line is shifted ($\Delta E_0 = 0$) because the theory predicts that line shape will be asymmetrical with a width $\Gamma_L + \Gamma_K$ on the low-energy side ($\Delta E_0 < 0$) and width Γ_L on the high-energy side.

In Fig. 2(b) the effect of the finite resolution of input energy would be to smear the theoretical curve and make its dip about 0.9 eV broader. The effect of finite resolution of the double-crystal Bragg spectrometer would be to increase the value of the observed linewidth by about 0.8 eV above the theoretical predictions. A more exact treatment can be made by actually convoluting the theory with the experimental resolution functions. In view of the poor signal-to-noise ratio such a procedure would seem unwarranted. The qualitative description of the effects of finite resolution is adequate enough to state that within our signal-to-noise ratio, theory and experiment agree.

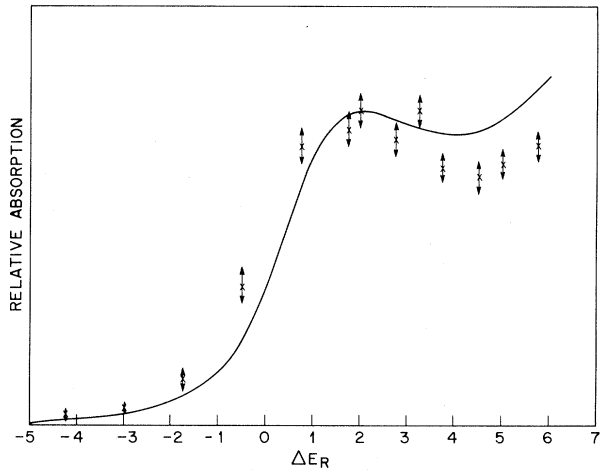

FIG. 3. The near-edge structure observed in Cu transmission studies (line) and the integrated 90° scattering intensity (points) as a function of ΔE_R. The slight saturation of the points in the strong-absorption region is due to finite penetration effects of the incident beam.

The physical picture that emerges for the resonant Raman regime removes the lifetime smearing of the K-hole intermediate state. This is exactly analogous to the situation in a two-level system with resonant excitation by a photon beam of energy width less than the lifetime width of the two levels. There one expects, as has recently been observed,[6] a line whose width is determined by the excitation beam width and not the lifetime width.

While it is true, as remarked by others,[7,8] that both fluorescence and resonant Raman scattering are describable by a single formula, the asymmetry in the density of empty states caused by the existence of the Fermi discontinuity does provide a clear transition point for distinguishing between the properties usually associated with absorption followed by emission and those associated with resonant Raman scattering. Such a clear distinction does not exist for the case of a sharp isolated upper state. In that case one can describe the observed phenomena either in terms of absorption into the tails of a lifetime-broadened transition followed by emission or as a resonantly enhanced scattering process in which the intermediate state is off the energy shell but the final state preserves energy conservation. Both points of view always give a line of FWHM $2\Gamma_L$ centered at $\Delta E_R = \Delta E_0$.

This work has demonstrated the possibility of doing precise resonant scattering studies in the x-ray regime and using them to determine an exact value for the threshold energy in metals. It has also been able to probe a distinct physical case in which resonant scattering and absorption followed by emission are distinguishable with line narrowing one of the manifestions of the distinction.

[1]C. J. Sparks, Phys. Rev. Lett. 33, 262 (1974).
[2]T. B. Bannett and I. Freund, Phys. Rev. Lett. 34, 273 (1975).
[3]P. Eisenberger, P. M. Platzman, and H. Winick, Phys. Rev. B (to be published).
[4]D. L. Walters and C. P. Bhalla, Phys. Rev. A 3, 1919 (1971).
[5]C. E. Moore, *Atomic Energy Levels as Derived from Analyses of Optical Spectra*, National Bureau of Standards Circular No. 467 (U. S. GPO, Washington, D. C., 1949), Vol. 1.
[6]F. Y. Wu, R. E. Grove, and S. Ezekiel, Phys. Rev. Lett. 35, 1426 (1975).
[7]Y. R. Shen, Phys. Rev. B 9, 622 (1974).
[8]J. R. Solin and H. Merkelo, Phys. Rev. B 12, 624 (1975).

COMMENTS

Comment on Plasmon Linewidth Experiments for Electrons on a Helium Surface

P. M. Platzman and G. Beni
Bell Laboratories, Murray Hill, New Jersey 07974
(Received 12 January 1976)

We show that the proper application of the established theory of electron-ripplon scattering for electrons trapped on helium correctly predicts the absolute linewidth, as a function of external electric field, observed in a recent plasmon experiment.

Electrons trapped on the surface of liquid helium form an almost perfect two-dimensional electron gas.[1,2] A recent experiment of Grimes and Adams[3] has graphically demonstrated the existence of long-wavelength two-dimensional plasmons propagating in this gas. In the regime below 0.6°K they were able to show that the plasmon lifetime was dominated by ripplon scattering and that the lifetime τ_{ac} appearing in a Drude fit to the high-frequency conductivity,

$$\sigma = \frac{ne^2}{im(\omega + i/\tau)} \simeq \frac{ne^2}{im\omega}\left(1 - \frac{i}{\omega\tau_{ac}}\right), \tag{1}$$

was empirically fitted by a function of the form

$$\tau_{ac}^{-1} = (eE_0 + eE_\perp)^2/C\ , \tag{2}$$

with

$$C \simeq 4\sigma_0\hbar\ , \tag{3}$$

where $\sigma_0 = 0.36$ erg/cm^2 is the surface tension, and with

$$E_0 \simeq 230 \pm 12\ \text{V/cm} \tag{4}$$

at $T = 0.5$°K. In Eq. (2) $E_\perp$ is the perpendicular electric field at the surface of the helium, which, along with the attractive image potentials and the 1-eV barrier preventing electrons from entering the helium, keeps a finite concentration, n, of them ($10^6 < n < 10^9$ cm^{-2}) at the surface.

Several workers[4,5] have attempted to calculate electron transport properties in the ripplon-dominated regime. The value of the temperature-independent high-field ripplon mobility for a thick film is given in Ref. 4 as

$$\mu_0 = \frac{8\sigma_0\hbar}{e^2E_\perp^2}\ \frac{e}{m} = \frac{e\tau_{dc}}{m}\ . \tag{5}$$

Grimes and Adams were quick to point out that $\tau_{dc} = 2\tau_{ac}$; i.e., there was an apparent disagreement. In addition they said that E_0 had not been calculated at all. In this Comment we would like to show that the theory of Shikin and Monarkha,[4] when properly applied to the problem of plasmon linewidth, yields precisely (no adjustable parameters) the correct values for C and the correct